RESEARCH ARTICLE

tpHusion: An efficient tool for clonal pH determination in *Drosophila*

Avantika Gupta, **Hugo Stocker** *

Institute of Molecular Systems Biology, ETH Zürich, Zürich, Switzerland

* stocker@imsb.biol.ethz.ch

Abstract

Genetically encoded pH indicators (GEpHI) have emerged as important tools for investigating intracellular pH (pHi) dynamics in *Drosophila*. However, most of the indicators are based on the Gal4/UAS binary expression system. Here, we report the generation of a ubiquitously-expressed GEpHI. The fusion protein of super ecliptic pHluorin and FusionRed was cloned under the tubulin promoter (tpHusion) to drive it independently of the Gal4/UAS system. The function of tpHusion was validated in various tissues from different developmental stages of *Drosophila*. Differences in pHi were also indicated correctly in fixed tissues. Finally, we describe the use of tpHusion for comparative analysis of pHi in manipulated clones and the surrounding cells in epithelial tissues. Our findings establish tpHusion as a robust tool for studying pHi in *Drosophila*.

Introduction

Perturbations in intracellular pH (pHi) affect many cellular processes including cell growth, proliferation, differentiation, and metabolism [1]. Under normal conditions, pHi is maintained within a narrow physiological range, and deregulation of pHi is observed in various disease states. In contrast to regular physiology, a state of higher pHi than the extracellular pH (pHe) is conducive to the survival of tumor cells and metastatic progression [2]. Alterations in cytosolic pH have also been implicated to cause neurodegenerative diseases [3]. Exploration of pH dynamics can provide a better understanding of the fundamental cellular processes and help develop strategies for the prevention or treatment of human pathologies.

Over the last few decades, several techniques for pHi measurement have been established. These include the use of proton-permeable microelectrodes, NMR and fluorescence spectroscopy [4,5]. The pH-sensitive fluorescent dyes offer easy-to-use tools for pHi measurement. Although the generation of ratiometric pH probes could address certain shortcomings such as dye leakage, photobleaching and uneven loading of dyes, the application of these dyes is limited in specific cases including pHi analysis in whole-mount tissues because of heterogeneous dye uptake. Construction of the pH-sensitive GFP variant, pHluorin [6], has led to the development of genetically encoded pH indicators (GEpHIs) for pHi measurements in various cell types and organelles. In *Drosophila*, GEpHIs are typically based on the Gal4/UAS system-driven expression of the pH-sensitive superecliptic pHluorin (SEpHluorin) [7] and the pH-insensitive mCherry [8] in the region of interest [9–11]. Improved modifications of the sensors have also been described [12] but an organism-wide expression has not been exploited. This

restricts the ability to examine pHi during developmental processes or in clonal situations within the same tissue, which is one of the major benefits of using *Drosophila* as a model system.

Overexpression of the *Drosophila* Na⁺-H⁺ exchanger, Nhe2, increases pHi in the retina [13]. However, the absence of an internal GEpHI expression and imaging control necessitates the generation of fluorescence ratio to pH calibration curves for every experiment. Ubiquitous expression of the GEpHI with a ubiquitously-expressed Gal4 in combination with other means to produce clonal manipulations (FLP/FRT, LexA or Q system) could provide 'in-tissue' control for a more accurate interpretation of results. However, this approach can be complicated by the prevalent use of the Gal4/UAS system and its possible toxicity [14]. To address these issues, we developed a Gal4/UAS-independent and ubiquitously-expressed GEpHI, called tpHusion. We describe its application for evaluation of pHi dynamics in living and fixed tissues, as well as for clonal analysis.

Materials and methods

Generation of *tpHusion Act>CD2>Gal4* chromosome

The *tubulin-3'-trailer* was excised from the pKB342 plasmid (gift from Konrad Basler) using restriction sites XhoI and XbaI, and subcloned in-line with the *pHusion-HRas* sequence (gift from Gregory Macleod, [15]) in pJFRC14 vector [16] using BamHI and XbaI sites. The resulting *pHusion-HRas-tubulin-3'-trailer* sequence was excised by restriction digestion with NotI and XbaI and used to replace the *Gal4* sequence under the *tubulin* promoter sequence in the pT2-attB-Gal4 vector (gift from Konrad Basler) using Acc65I and XbaI sites. The resulting plasmid tpHusion was injected into the fly line ΦX-86Fb [17]. The *3xP3-RFPattP* landing site sequence was removed using Cre recombinase-mediated excision. The *Act>CD2>Gal4* construct was recombined on the resulting 3R chromosome arm to generate the *tpHusion Act>CD2>Gal4* chromosome.

Fly husbandry

All lines and crosses were maintained at 25˚C on normal fly food unless otherwise stated. Normal fly food is composed of 100 g fresh yeast, 55 g cornmeal, 10 g wheat flour, 75 g sugar, 8 g bacto agar, and 1.5% antimicrobial agents (33 g/L nipagin and 66 g/L nipasol in ethanol) in 1 L water.

Fly lines used: *ϕX-86Fb* (gift from Johannes Bischof), *Act>CD2>Gal4* (4780 Bloomington Drosophila Stock Center (BDSC)); *UAS-ECFP-golgi* (42710 BDSC), *UAS-LacZ* (control, gift from Johannes Bischof), *UAS-Ras^{V12}* [18], *Pten^{Ri}* (101475 Vienna Drosophila Resource Center (VDRC)), *foxo^{Ri}* (107786 VDRC), and *Tsc1^{Ri}* (31039 BDSC).

Cross setup and clone induction

Flies were crossed for two days before an overnight egg laying. For clone induction, a 15 min heat shock at 37˚C was applied 36 h after egg laying (AEL) and the animals were allowed to develop at 25˚C. Wing and eye imaginal discs, and brains were dissected from wandering L3 larvae 108 h AEL; ovarioles were dissected from fertilized females. For clonal analyses, only female larvae were used for dissection. Tissues were dissected in HCO_3^- buffer [19] for live imaging or in 4% paraformaldehyde (PFA) for fixed tissue imaging.

Microscopy and immunofluorescence staining

After dissection of live tissues in HCO_3^- buffer, the samples were mounted in the same buffer on 35 mm MatTek dishes coated with 0.1 mg/mL poly-L-Lysine. Fluorescence images were acquired on a Visitron Spinning Disk confocal microscope within one hour of dissection.

For fixed samples, tissues were dissected in 4% PFA, fixed for at least 30 min at room temperature (RT), and stored at 4°C until processing of all experimental conditions. The samples were washed in PBS for 10 min and mounted on glass slides in VECTASHIELD (Vector Laboratories H-1000) mounting medium. Confocal images were obtained within 24 h of dissection on a Leica SPE TCS confocal laser-scanning microscope.

For the immunofluorescence staining with Fasciclin III (FasIII), tissues were dissected in PBS. The samples were fixed in 4% PFA (30 min, RT), washed thrice in 0.3% Triton-X in PBS (PBT, 15 min, RT), blocked in 2% Normal Donkey Serum (NDS) in 0.3% PBT (2 h, 4°C), incubated with mouse anti-FasIII (1:15 in 2% NDS, 7G10 Developmental Studies Hybridoma Bank (DSHB), overnight, 4°C), washed thrice in 0.3% PBT (15 min each, RT), incubated with goat anti-mouse Alexa Fluor 647 (1:500, Thermo Fisher Scientific, 2 h, RT), washed thrice in 0.3% PBT (15 min each, RT), stained with DAPI in 0.3% PBT (1:2000, 10 min, RT), and washed once with PBS (10 min, RT). The samples were mounted on glass slides in VECTASHIELD and imaged using a Leica SPE TCS confocal laser-scanning microscope.

In vivo nigericin calibration

Nigericin calibration buffers and curves were generated as described previously [19]. Briefly, after acquiring images of live tissues, the HCO_3^- buffer was replaced with the first calibration buffer containing nigericin. Samples were imaged every 4 min after a minimum incubation of 10 min. After a total incubation time of 20 min, subsequent buffers were added for 6 min and images were acquired every 2 min.

Quantification and statistical analysis

Images were processed using ImageJ [20]. Background subtraction was performed for each channel. The images were converted to 32-bit and median filtering was applied with radius 2. A defined area encompassing cells of interest, clones or surrounding wild-type tissue was selected and mean gray values were measured for SEpHluorin and FusionRed. The pseudo color images were produced by auto-thresholding of individual channels, followed by division of SEpHluorin channel intensity with FusionRed. The calibration bar represents the relative ratio of SEpHluorin to FusionRed intensities within a tissue from low (blue) to high (red). Statistical analyses were performed using unpaired two-tailed Student's t-test. *p* values are described in the Figure legends. All plots were generated in R Studio and Figures were assembled using Adobe Illustrator.

Results

Development and *in vivo* validation of tpHusion pH reporter

The use of the Gal4/UAS system is one of the most common ways to produce clonal manipulations in *Drosophila* [21]. To develop a ubiquitously-expressed GEpHI that would be useful for clonal analysis, the expression of the sensor was rendered independent of Gal4/UAS control. A translational fusion protein of SEpHluorin with FusionRed was cloned under the control of the *tubulin* promoter. FusionRed was used to replace mCherry due to its low cytotoxicity, better performance in fusions and increased stability in a monomeric state [22]. An *HRas* sequence was also included to tether the fusion protein to the cytosolic side of the plasma

membrane. This reduces the pHi variability due to the presence of compartments of differing pH within the cytosol [23]. The construct is referred to as tpHusion. The expression and membrane localization of tpHusion was confirmed in various tissues (data shown for wing imaginal discs in Fig 1A).

To verify that tpHusion is a suitable pH indicator, fluorescence intensity calibrations were performed on wing imaginal discs incubated in buffers containing nigericin, which is an ionophore used to clamp the pHi to the buffer pH (see Materials and Methods). The pH-sensitive SEpHluorin displayed the predicted changes in fluorescence based on the buffer pH, whereas the pH-insensitive FusionRed only showed minor alterations. The ratio of SEpHluorin to FusionRed reflected the buffer pH (Fig 1B), resulting in the generation of a calibration curve of pHi with the ratio of fluorescence intensities (Fig 1C). Thus, tpHusion can be used to indicate changes in pHi.

## tpHusion reports pHi changes in living tissues

Apart from the clonal analyses, a major advantage of a ubiquitously-expressed GEpHI is the ability to compare pHi in different cells across various developmental processes and stages. Earlier studies have reported a higher pHi in the differentiated follicle cells of the *Drosophila* ovariole as compared to the follicle stem cells (FSCs) using the Gal4/UAS-dependent expression of SEpHluorin/mCherry probe [24]. This finding was confirmed using tpHusion, which showed a similar increase in pHi of follicle cells in contrast to the FSCs (Fig 2A and 2A').

The *Drosophila* imaginal discs have proven to be excellent systems for the identification of genes regulating cellular growth during normal development [25,26] or in perturbed states [27,28]. The pHi in these tissues has not been analyzed due to the unavailability of robust indicators. During the larval stages, the eye imaginal disc consists of proliferating cells anterior to the morphogenetic furrow (amf) and mostly differentiating photoreceptors posterior to the furrow (pmf) [29]. Investigation of SEpHluorin and FusionRed intensities using tpHusion demonstrated a higher ratio in the mitotically active amf region of the eye disc (Fig 2B and 2B'). The several compartments and cell lineages of the wing disc have also been described in great detail [26]. The larval wing disc is comprised of cells in the pouch region (which will form the wing blade) and the notum (which will form the body wall) [30,31]. pHi analysis using tpHusion displayed no difference in the pouch versus notum of the wing imaginal disc (Fig 2C and 2C').

A major organ that is vital in neurobiological research is the *Drosophila* brain [32]. Tremendous advances have been made towards deciphering the circuitries of the adult and larval brains [33,34]. The information about pHi of different cell types could be fundamental to understand processes such as vesicular transport [35]. The larval brain can be subdivided into the central brain (CB), optic lobe (OL) and the ventral nerve cord (VNC) [36]. A brief evaluation in the larval brain revealed that cells in the OL have a higher pHi than cells in the CB (Fig 2D and 2D'). The above results establish the use of tpHusion for comparative analysis of *in vivo* pH differences in various *Drosophila* tissues during different developmental stages.

tpHusion reflects *in vivo* pH changes in fixed tissues

Culturing of *Drosophila* organs has been challenging, with specific culture condition requirements for different tissues [37–40]. For pHi measurements in live cells, tissues are dissected in a bicarbonate buffer (see Materials and Methods) to prevent changes in the physiological pHi. However, the tissues cannot be maintained in this buffer for an extended period, rendering the handling of many experimental conditions difficult. Fixing the conformational state of the GEpHI can help slow down changes in fluorescence until all samples are processed [41]. To
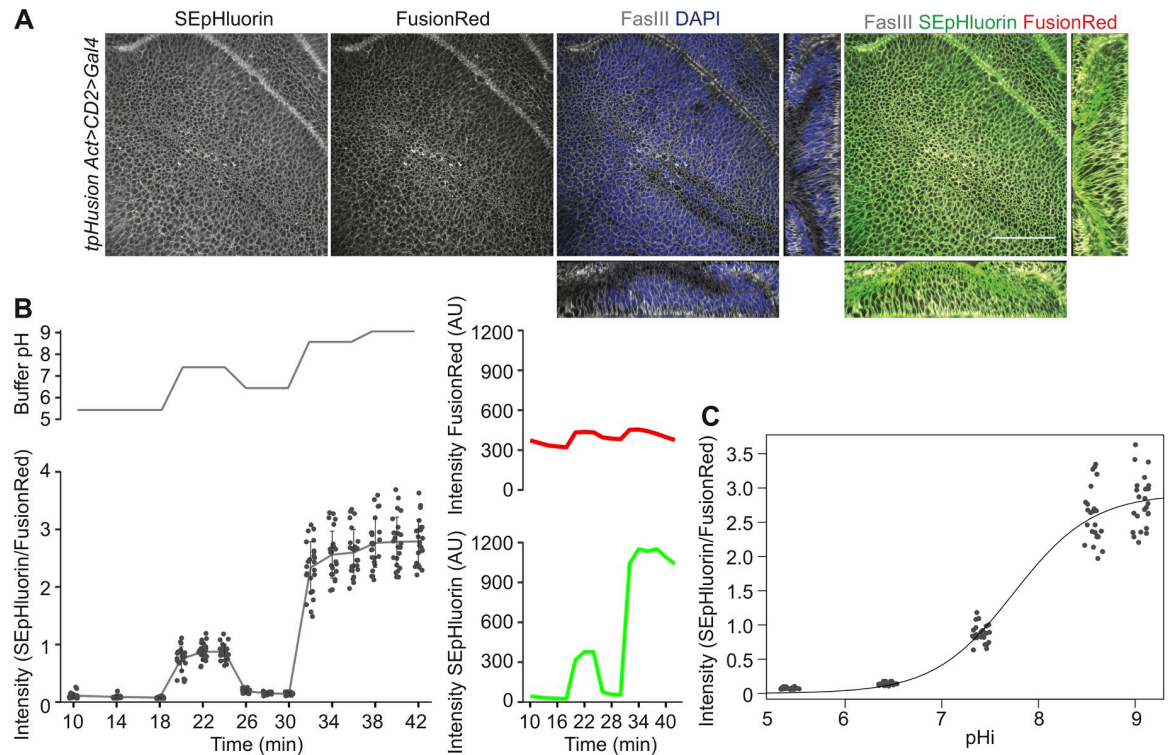
Fig 1. Validation of tpHusion reporter. (A) Fixed wing pouches of wandering L3 larvae depicting the cellular localization of tpHusion. FasIII labels the plasma membrane and DAPI stains the nuclei. Scale bar = 50 μm. (B) Changes in SEpHluorin (green) and FusionRed (red) fluorescence intensities, and the ratio of SEpHluorin to FusionRed intensities from live wing pouch cells upon incubation in nigericin buffers of varying pH. n > 7 larvae. Data are represented as mean ± standard deviation. (C) Calibration curve between intracellular pH (pHi) and the ratio of SEpHluorin to FusionRed intensities generated from experiments in B.

examine if tpHusion can be used to monitor pH variations in fixed tissues, comparisons were performed in tissue regions depicted in Fig 2 after fixation. The tissues were dissected directly in 4% PFA to restrict changes in pHi and imaged within 24 h. Interestingly, differences in the ratio of SEpHluorin and FusionRed intensities in the various cell types of the tissues tested were the same as in the live tissues (Fig 3A–3D'). SEpHluorin retains sensitivity to acidic pH after fixation [42]. Since the samples were exclusively exposed to pH 7–7.4 in our experimental setup, the physiological pHi should be maintained. This does not exclude the possibility of slight alterations in pHi but the consistent changes in the ratio of intensities between different regions of the live and fixed tissues (compare Figs 2 and 3) suggest that tpHusion can be reliably used to study pHi variations in fixed tissues.

## Using tpHusion to detect clonal pH changes

Deregulated pH is now considered a hallmark of cancer with a higher pHi and a lower pHe observed in cancer cells as compared to normal cells [43]. Many tumor models have been described in *Drosophila* [44]. Overexpression of activated Ras (*Ras^{V12}*) causes hyperplastic overgrowth [45] and metastatic behavior in combination with loss of polarity genes [27]. It has also been shown to have an increased pHi compared to control cells in a 2D cell culture system of breast epithelial cells [13]. To analyze the pHi in *Ras^{V12}*-overexpressing clones in *Drosophila* epithelial cells, tpHusion was recombined with an actin-FLP-out cassette [46]. Comparison of SEpHluorin and FusionRed intensities ratio in clones and the surrounding wild-type tissue revealed an elevated pHi in the clones (Fig 4A and 4A').
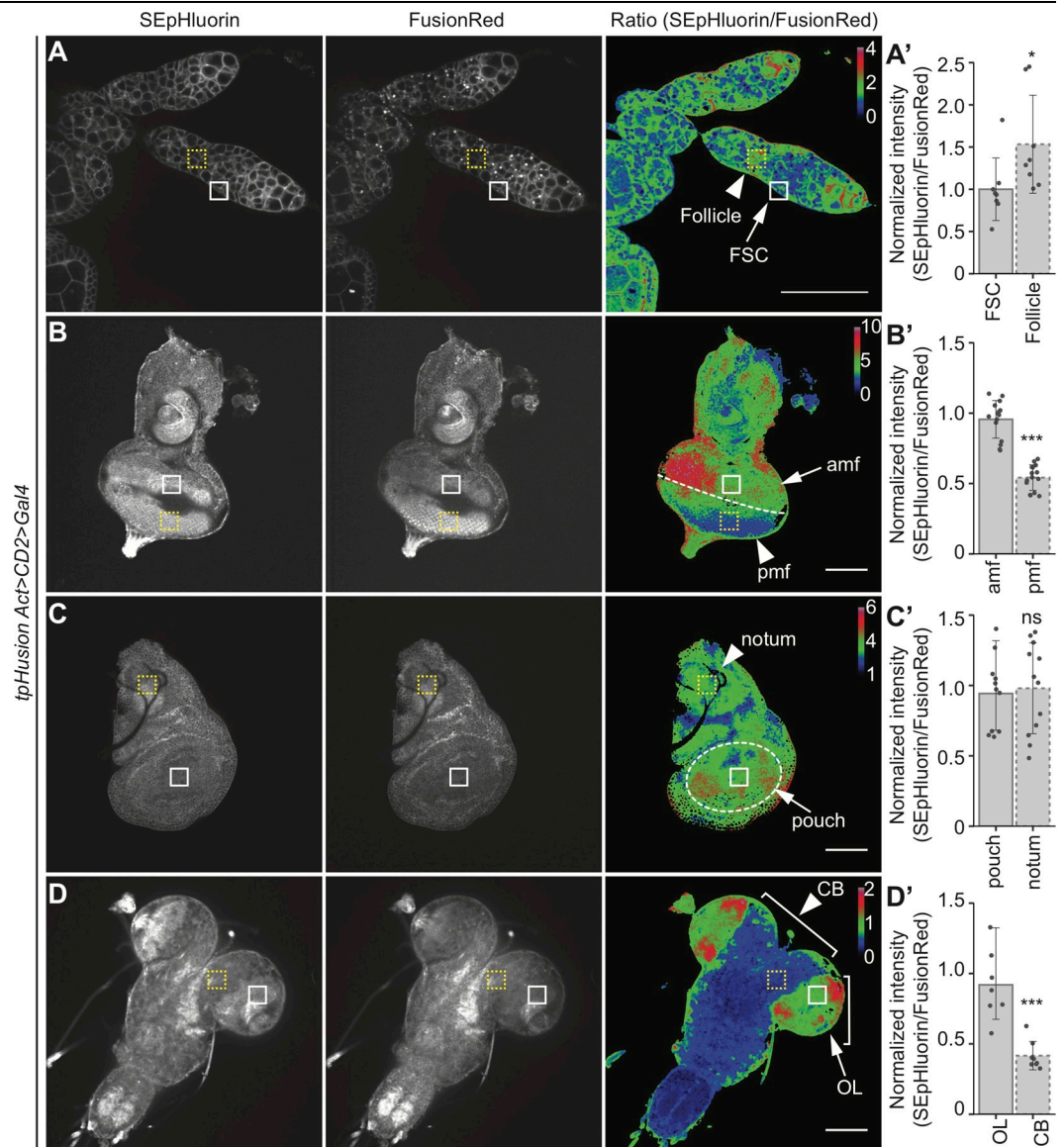
Fig 2. Comparison of pHi in different cell types of living tissues. (A-D) SEpHluorin, FusionRed, and ratiometric images of live (A) ovarioles, (B) eye discs, (C) wing discs, and (D) brains. (A'-D') Quantification of the ratio of fluorescence intensities in (A') FSC (arrow, white solid square) and follicle (arrowhead, yellow dashed square) cells, (B') cells anterior (amf, arrow, white solid square) and posterior (pmf, arrowhead, yellow dashed square) to the morphogenetic furrow (dashed line), (C') pouch (arrow, white solid square) and notum (arrowhead, yellow dashed square) cells, and (D') cells in optic lobe (OL, arrow, white solid square) and central brain (CB, arrowhead, yellow dashed square). n > 7 larvae. Data are represented as mean ± standard deviation. * $p < 0.05$, *** $p < 0.001$ and ns = not significant. Scale bar for A = 50 μm, scale bar for B-D = 100 μm. Calibration bar represents the ratio values of SEpHluorin to FusionRed intensities used to generate ratiometric images.

https://doi.org/10.1371/journal.pone.0228995.g002

Earlier studies have reported an enhanced cellular overgrowth upon clonal loss of tumor suppressors of the phosphatidylinositol 3-kinase (PI3K)/Akt/mechanistic target of rapamycin (mTORC1) signaling network. Loss-of-function mutations in the phosphatase and tensin homolog (Pten) or the tuberous sclerosis complex (TSC) subunit 1 (Tsc1) lead to an escalation in cell size and number [47,48]. We have also outlined the function of the transcription factor forkhead box O (FoxO) in limiting the proliferation of *Tsc1* mutant cells under conditions of nutrient restriction [49]. The loss of *foxo* does not cause an overgrowth phenotype on its own
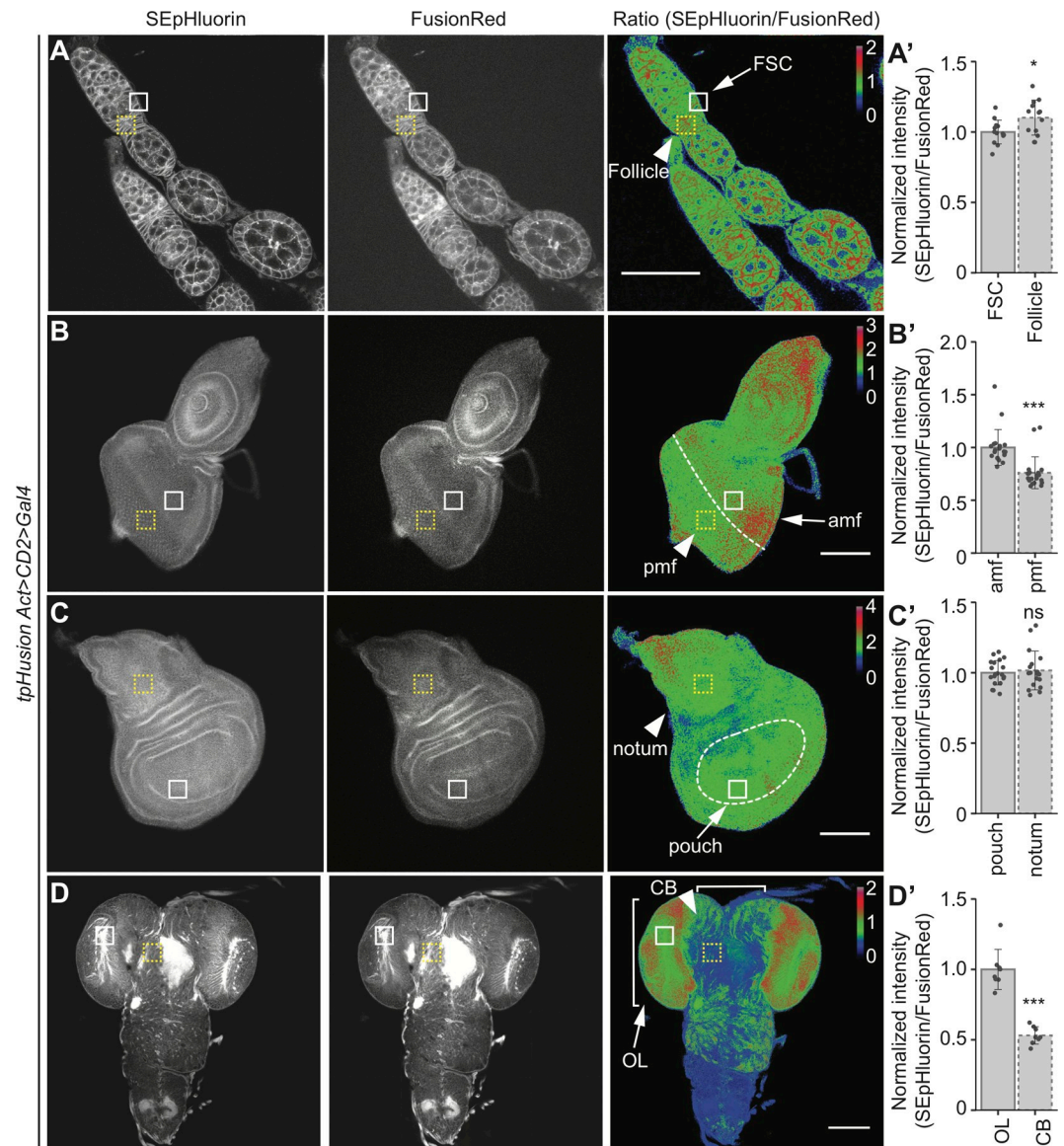
Fig 3. Comparison of pHi in different cell types of fixed tissues. (A-D) SEpHluorin, FusionRed, and ratiometric images of fixed (A) ovarioles, (B) eye discs, (C) wing discs, and (D) brains. (A'-D') Quantification of the ratio of fluorescence intensities in (A') FSC (arrow, white solid square) and follicle (arrowhead, yellow dashed square) cells, (B') cells anterior (amf, arrow, white solid square) and posterior (pmf, arrowhead, yellow dashed square) to the morphogenetic furrow (dashed line), (C') pouch (arrow, white solid square) and notum (arrowhead, yellow dashed square) cells, and (D') cells in optic lobe (OL, arrow, white solid square) and central brain (CB, arrowhead, yellow dashed square). n > 7 larvae. Data are represented as mean ± standard deviation. * $p < 0.05$, *** $p < 0.001$ and ns = not significant. Scale bar for A = 50 μm, scale bar for B-D = 100 μm. Calibration bar represents the ratio values of SEpHluorin to FusionRed intensities used to generate ratiometric images.

[50]. Using the system mentioned above, the pHi of control, *Pten*, *foxo*, *Tsc1*, and *Tsc1 foxo* knockdown clones was compared to the surrounding wild-type tissue (Fig 4B). The ratio of SEpHluorin and FusionRed intensities in control and *foxo* knockdown clones was similar to the surrounding wild-type tissue, whereas the ratio was higher in *Pten*, *Tsc1*, and *Tsc1 foxo* knockdown clones. These data validate the use of tpHusion for clonal analysis of pHi in *Drosophila* epithelial tissues and suggest that loss of the tested tumor suppressors increases pHi.
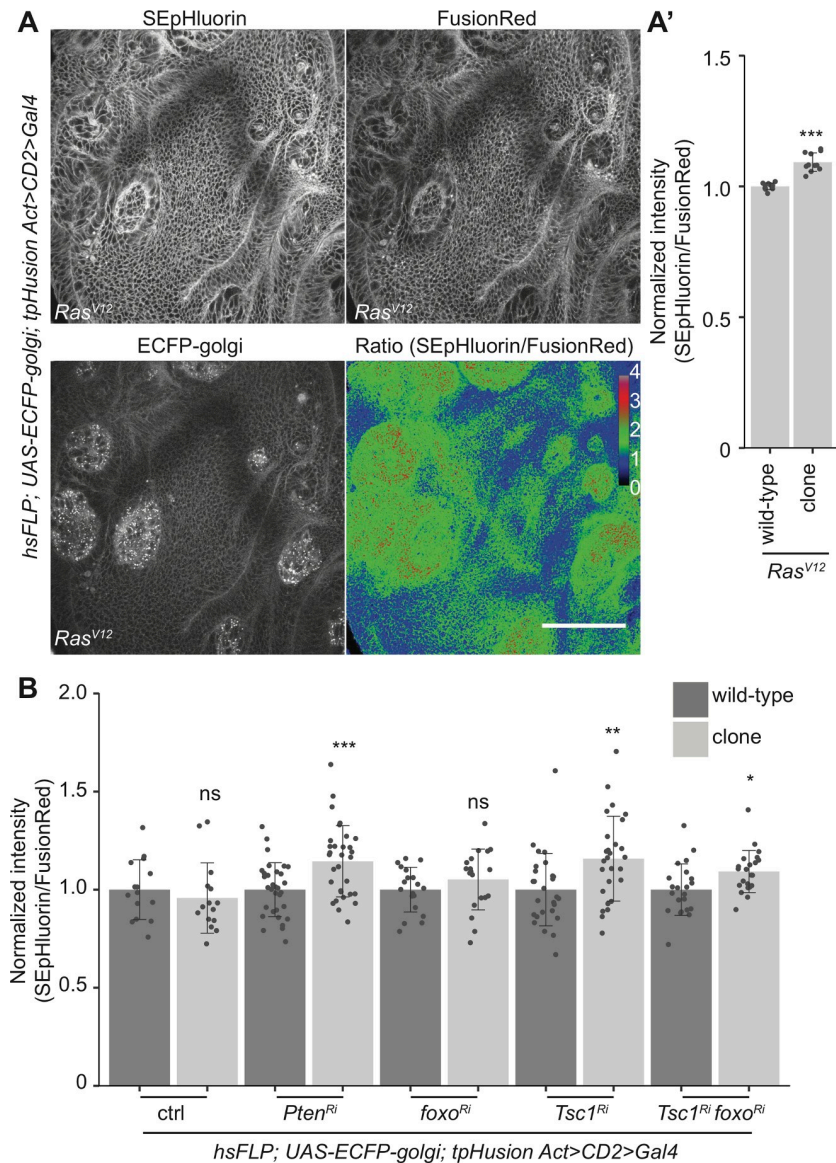
Fig 4. tpHusion detects clonal pH changes in *Drosophila* imaginal discs. (A) SEpHluorin, FusionRed and ratiometric images of wing pouches dissected from wandering female L3 larvae with *Ras^V12*-overexpressing clones that are marked by ECFP. Calibration bar represents the ratio values of SEpHluorin to FusionRed intensities used to generate ratiometric images. Scale bar = 50 μm. (A') Quantification of the ratio of fluorescence intensities in wild-type and *Ras^V12* clones. (B) Quantification of the ratio of fluorescence intensities in wild-type and control, *Pten^Ri*, *foxo^Ri*, *Tsc1^Ri* or *Tsc1^Ri foxo^Ri* clones from wing pouches of wandering female L3 larvae. n > 10 larvae. Data are represented as mean ± standard deviation. * $p < 0.05$, ** $p < 0.01$, *** $p < 0.001$ and ns = not significant.

https://doi.org/10.1371/journal.pone.0228995.g004

Discussion

The ubiquitously-expressed GEpHI, tpHusion, facilitates *in vivo* pHi measurement and comparative analysis in diverse tissues and developmental stages in *Drosophila*. We have used this reporter to investigate pHi differences in developing organs and genetically manipulated clones compared to their surrounding cells in the same tissue.

Such an analysis was not feasible with the previously available tools for pHi determination. Our results demonstrate the applicability of tpHusion for the identification of new pHi modulators, and for studying pHi homeostasis during developmental processes or in disease models.

Minor imbalances in the intracellular and extracellular pH equilibrium can have major impacts on many cellular functions. The regulation of cell proliferation by pHi has been shown in a variety of species including sea urchin eggs, yeast, and mammalian cell culture systems [51]. Changing pHi can coordinate differentiation or lineage specification of certain stem cells [24,52,53]. pHi has also been found to change during cell cycle progression [54]. Given the crucial role of pH in physiology, it is not surprising that a loss of pH homeostasis is seen in many diseases including cancer [55]. One notable aspect of this observation that remains disputed in the field is if pH can signal to cellular processes leading to diseases or whether the observed pH imbalance is a result of the pathological state.

Studies addressing the role of pHi in the fundamental processes mentioned above have been limited in *Drosophila* due to the lack of adequate tools. The uniform expression of tpHusion with no apparent cytotoxicity throughout development can aid the analysis of pHi dynamics in various developmental contexts. The complete potential of tpHusion can be realized by combining it with the existing repertoire of genetic modification tools in *Drosophila*. The flexible use of tpHusion with the Gal/UAS and FLP-out systems to express UAS-based transgenes in clones led us to present, for the first time, an increase in pHi in cells with overexpression of an oncogene or knockdown of tumor suppressor genes as compared to the surrounding wild-type cells. One caveat is the inability to use the most commonly used fluorophores to label clones or cell lineages but this can be circumvented by the use of non-interfering fluorophores in the blue or the far-red channels. We conclude that tpHusion is a powerful tool for investigating cellular pH in *Drosophila*.

Acknowledgments

Author Contributions

Conceptualization: Avantika Gupta, Hugo Stocker.

Formal analysis: Avantika Gupta.

Funding acquisition: Hugo Stocker.

Investigation: Avantika Gupta.

Methodology: Avantika Gupta.

Supervision: Hugo Stocker.

Writing – original draft: Avantika Gupta.

Writing – review & editing: Hugo Stocker.

References

1. Srivastava J, Barber DL, Jacobson MP. Intracellular pH Sensors: Design Principles and Functional Significance. Physiology. 2007 Feb; 22(1):30–9.

2. Webb BA, Chimenti M, Jacobson MP, Barber DL. Dysregulated pH: a perfect storm for cancer progression. Nat Rev Cancer. 2011 Sep 11; 11(9):671–7. https://doi.org/10.1038/nrc3110 PMID: 21833026

3. Majdi A, Mahmoudi J, Sadigh-Eteghad S, Golzari SEJ, Sabermarouf B, Reyhani-Rad S. Permissive role of cytosolic pH acidification in neurodegeneration: A closer look at its causes and consequences. J Neurosci Res. 2016 Oct; 94(10):879–87. https://doi.org/10.1002/jnr.23757 PMID: 27282491

4. Loiselle FB, Casey JR. Measurement of Intracellular pH. In: Methods in molecular biology (Clifton, NJ). 2010. p. 311–31.

5. Han J, Burgess K. Fluorescent Indicators for Intracellular pH. Chem Rev. 2010 May 12; 110(5):2709–28. https://doi.org/10.1021/cr900249z PMID: 19831417

6. Miesenböck G, De Angelis DA, Rothman JE. Visualizing secretion and synaptic transmission with pH-sensitive green fluorescent proteins. Nature. 1998 Jul; 394(6689):192–5. https://doi.org/10.1038/28190 PMID: 9671304

7. Sankaranarayanan S, De Angelis D, Rothman JE, Ryan TA. The Use of pHluorins for Optical Measurements of Presynaptic Activity. Biophys J. 2000 Oct; 79(4):2199–208. https://doi.org/10.1016/S0006-3495(00)76468-X PMID: 11023924

8. Koivusalo M, Welch C, Hayashi H, Scott CC, Kim M, Alexander T, et al. Amiloride inhibits macropinocytosis by lowering submembranous pH and preventing Rac1 and Cdc42 signaling. J Cell Biol. 2010 Feb 22; 188(4):547–63. https://doi.org/10.1083/jcb.200908086 PMID: 20156964

9. Poskanzer KE, Marek KW, Sweeney ST, Davis GW. Synaptotagmin I is necessary for compensatory synaptic vesicle endocytosis in vivo. Nature. 2003 Dec 23; 426(6966):559–63. https://doi.org/10.1038/nature02184 PMID: 14634669

10. Rossano AJ, Chouhan AK, Macleod GT. Genetically encoded pH-indicators reveal activity-dependent cytosolic acidification of Drosophila motor nerve termini in vivo. J Physiol. 2013 Apr 1; 591(7):1691–706. https://doi.org/10.1113/jphysiol.2012.248377 PMID: 23401611

11. Harris KP, Zhang YV, Piccioli ZD, Perrimon N, Littleton JT. The postsynaptic t-SNARE Syntaxin 4 controls traffic of Neuroligin 1 and Synaptotagmin 4 to regulate retrograde signaling. Elife. 2016 May 25;5.

12. Rossano AJ, Kato A, Minard KI, Romero MF, Macleod GT. Na + /H + exchange via the Drosophila vesicular glutamate transporter mediates activity-induced acid efflux from presynaptic terminals. J Physiol. 2017 Feb 1; 595(3):805–24. https://doi.org/10.1113/JP273105 PMID: 27641622

13. Grillo-Hill BK, Choi C, Jimenez-Vidal M, Barber DL. Increased H+ efflux is sufficient to induce dysplasia and necessary for viability with oncogene expression. Elife. 2015 Mar 20;4.

14. Kramer JM, Staveley BE. GAL4 causes developmental defects and apoptosis when expressed in the developing eye of Drosophila melanogaster. Genet Mol Res. 2003; 2(1):43–7. PMID: 12917801

15. Stawarski M, Hernandez RX, Feghhi T, Borycz JA, Lu Z, Agarwal A, et al. Neuronal glutamatergic synaptic clefts alkalinize rather than acidify during neurotransmission. J. Neurosci. 2020; https://doi.org/10.1523/JNEUROSCI.1774-19.2020 PMID: 31964719

16. Pfeiffer BD, Ngo T-TB, Hibbard KL, Murphy C, Jenett A, Truman JW, et al. Refinement of Tools for Targeted Gene Expression in Drosophila. Genetics. 2010 Oct; 186(2):735–55. https://doi.org/10.1534/genetics.110.119917 PMID: 20697123

17. Bischof J, Maeda RK, Hediger M, Karch F, Basler K. An optimized transgenesis system for Drosophila using germ-line-specific C31 integrases. Proc Natl Acad Sci. 2007 Feb 27; 104(9):3312–7. https://doi.org/10.1073/pnas.0611511104 PMID: 17360644

18. Halfar K, Rommel C, Stocker H, Hafen E. Ras controls growth, survival and differentiation in the Drosophila eye by different thresholds of MAP kinase activity. Development. 2001; 128(9):1687–96. PMID: 11290305

19. Grillo-Hill BK, Webb BA, Barber DL. Ratiometric Imaging of pH Probes. In: Methods in Cell Biology. 2014. p. 429–48. https://doi.org/10.1016/B978-0-12-420138-5.00023-9 PMID: 24974041

20. Schindelin J, Arganda-Carreras I, Frise E, Kaynig V, Longair M, Pietzsch T, et al. Fiji: an open-source platform for biological-image analysis. Nat Methods. 2012 Jul 28; 9(7):676–82. https://doi.org/10.1038/nmeth.2019 PMID: 22743772

21. Yagi R, Mayer F, Basler K. Refined LexA transactivators and their use in combination with the Drosophila Gal4 system. Proc Natl Acad Sci. 2010 Sep 14; 107(37):16166–71. https://doi.org/10.1073/pnas.1005957107 PMID: 20805468

22. Shemiakina II, Ermakova GV, Cranfill PJ, Baird MA, Evans RA, Souslova EA, et al. A monomeric red fluorescent protein with low cytotoxicity. Nat Commun. 2012 Jan 13; 3(1):1204.

23. Benčina M. Illumination of the Spatial Order of Intracellular pH by Genetically Encoded pH-Sensitive Sensors. Sensors. 2013 Dec 5; 13(12):16736–58. https://doi.org/10.3390/s131216736 PMID: 24316570

24. Ulmschneider B, Grillo-Hill BK, Benitez M, Azimova DR, Barber DL, Nystul TG. Increased intracellular pH is necessary for adult epithelial and embryonic stem cell differentiation. J Cell Biol. 2016 Nov 7; 215 (3):345–55. https://doi.org/10.1083/jcb.201606042 PMID: 27821494

25. St Johnston D. The art and design of genetic screens: Drosophila melanogaster. Nat Rev Genet. 2002 Mar; 3(3):176–88. https://doi.org/10.1038/nrg751 PMID: 11972155

26. Hariharan IK. Organ Size Control: Lessons from Drosophila. Dev Cell. 2015 Aug; 34(3):255–65. https://doi.org/10.1016/j.devcel.2015.07.012 PMID: 26267393

27. Pagliarini RA. A Genetic Screen in Drosophila for Metastatic Behavior. Science (80-). 2003 Nov 14; 302 (5648):1227–31. https://doi.org/10.1126/science.1088474 PMID: 14551319

28. Hariharan IK, Serras F. Imaginal disc regeneration takes flight. Curr Opin Cell Biol. 2017 Oct; 48:10–6. https://doi.org/10.1016/j.ceb.2017.03.005 PMID: 28376317

29. Treisman JE. Retinal differentiation in Drosophila. Wiley Interdiscip Rev Dev Biol. 2013 Jul; 2(4):545–57. https://doi.org/10.1002/wdev.100 PMID: 24014422

30. Diaz de la Loza MC, Thompson BJ. Forces shaping the Drosophila wing. Mech Dev. 2017 Apr; 144:23–32. https://doi.org/10.1016/j.mod.2016.10.003 PMID: 27784612

31. Zecca M, Struhl G. Subdivision of the Drosophila wing imaginal disc by EGFR-mediated signaling. Development. 2002; 129(6):1357–68. PMID: 11880345

32. Scheffer LK, Meinertzhagen IA. The Fly Brain Atlas. Annu Rev Cell Dev Biol. 2019 Oct 6; 35(1):637–53.

33. Shih C-T, Sporns O, Yuan S-L, Su T-S, Lin Y-J, Chuang C-C, et al. Connectomics-Based Analysis of Information Flow in the Drosophila Brain. Curr Biol. 2015 May; 25(10):1249–58. https://doi.org/10.1016/j.cub.2015.03.021 PMID: 25866397

34. Eichler K, Li F, Litwin-Kumar A, Park Y, Andrade I, Schneider-Mizell CM, et al. The complete connectome of a learning and memory centre in an insect brain. Nature. 2017 Aug 10; 548(7666):175–82. https://doi.org/10.1038/nature23455 PMID: 28796202

35. Freyberg Z, Sonders MS, Aguilar JI, Hiranita T, Karam CS, Flores J, et al. Mechanisms of amphetamine action illuminated through optical monitoring of dopamine synaptic vesicles in Drosophila brain. Nat Commun. 2016 Apr 16; 7(1):10652.

36. Ramon-Cañellas P, Peterson HP, Morante J. From Early to Late Neurogenesis: Neural Progenitors and the Glial Niche from a Fly's Point of View. Neuroscience. 2019 Feb; 399:39–52. https://doi.org/10.1016/j.neuroscience.2018.12.014 PMID: 30578972

37. Zartman J, Restrepo S, Basler K. A high-throughput template for optimizing Drosophila organ culture with response-surface methods. Development. 2013 Feb 1; 140(3):667–74. https://doi.org/10.1242/dev.088872 PMID: 23293298

38. Handke B, Szabad J, Lidsky PV, Hafen E, Lehner CF. Towards Long Term Cultivation of Drosophila Wing Imaginal Discs In Vitro. Kango-Singh M, editor. PLoS One. 2014 Sep 9; 9(9):e107333. https://doi.org/10.1371/journal.pone.0107333 PMID: 25203426

39. Tsao C-K, Ku H-Y, Lee Y-M, Huang Y-F, Sun YH. Long Term Ex Vivo Culture and Live Imaging of Drosophila Larval Imaginal Discs. Bergmann A, editor. PLoS One. 2016 Sep 29; 11(9):e0163744. https://doi.org/10.1371/journal.pone.0163744 PMID: 27685172

40. Peters NC, Berg CA. In Vitro Culturing and Live Imaging of Drosophila Egg Chambers: A History and Adaptable Method. In: Methods in Molecular Biology. 2016. p. 35–68.

41. Delloye-Bourgeois C, Jacquier A, Falk J, Castellani V. Use of pHluorin to Assess the Dynamics of Axon Guidance Receptors in Cell Culture and in the Chick Embryo. J Vis Exp. 2014 Jan 12;(83).

42. Tanida I, Ueno T, Uchiyama Y. A Super-Ecliptic, pHluorin-mKate2, Tandem Fluorescent Protein-Tagged Human LC3 for the Monitoring of Mammalian Autophagy. Bassham D, editor. PLoS One. 2014 Oct 23; 9(10):e110600. https://doi.org/10.1371/journal.pone.0110600 PMID: 25340751

43. White KA, Kisor K, Barber DL. Intracellular pH dynamics and charge-changing somatic mutations in cancer. Cancer Metastasis Rev. 2019 Jun 13; 38(1–2):17–24. https://doi.org/10.1007/s10555-019-09791-8 PMID: 30982102

44. Mirzoyan Z, Sollazzo M, Allocca M, Valenza AM, Grifoni D, Bellosta P. Drosophila melanogaster: A Model Organism to Study Cancer. Front Genet. 2019 Mar 1; 10.

45. Karim FD, Rubin GM. Ectopic expression of activated Ras1 induces hyperplastic growth and increased cell death in Drosophila imaginal tissues. Development. 1998; 125(1):1–9. PMID: 9389658

46. Struhl G, Basler K. Organizing activity of wingless protein in Drosophila. Cell. 1993 Feb; 72(4):527–40. https://doi.org/10.1016/0092-8674(93)90072-x PMID: 8440019

47. Goberdhan DCI, Paricio N, Goodman EC, Mlodzik M, Wilson C. Drosophila tumor suppressor PTEN controls cell size and number by antagonizing the Chico/PI3-kinase signaling pathway. Genes Dev. 1999 Dec 15; 13(24):3244–58. https://doi.org/10.1101/gad.13.24.3244 PMID: 10617573

48. Tapon N, Ito N, Dickson BJ, Treisman JE, Hariharan IK. The Drosophila Tuberous Sclerosis Complex Gene Homologs Restrict Cell Growth and Cell Proliferation. Cell. 2001 May; 105(3):345–55. https://doi.org/10.1016/s0092-8674(01)00332-4 PMID: 11348591

49. Nowak K, Gupta A, Stocker H. FoxO restricts growth and differentiation of cells with elevated TORC1 activity under nutrient restriction. PLoS Genet. 2018; 14(4):e1007347. https://doi.org/10.1371/journal.pgen.1007347 PMID: 29677182

50. Junger MA, Rintelen F, Stocker H, Wasserman JD, Vegh M, Radimerski T, et al. The Drosophila forkhead transcription factor FOXO mediates the reduction in cell number associated with reduced insulin signaling. J Biol. 2003; 2(3):20. https://doi.org/10.1186/1475-4924-2-20 PMID: 12908874

51. Flinck M, Kramer SH, Pedersen SF. Roles of pH in control of cell proliferation. Acta Physiol. 2018 Jul; 223(3):e13068.

52. Li X, Karki P, Lei L, Wang H, Fliegel L. Na + /H + exchanger isoform 1 facilitates cardiomyocyte embryonic stem cell differentiation. Am J Physiol Circ Physiol. 2009 Jan; 296(1):H159–70.

53. Gao W, Zhang H, Chang G, Xie Z, Wang H, Ma L, et al. Decreased Intracellular pH Induced by Cariporide Differentially Contributes to Human Umbilical Cord-Derived Mesenchymal Stem Cells Differentiation. Cell Physiol Biochem. 2014; 33(1):185–94. https://doi.org/10.1159/000356661 PMID: 24481225

54. Putney LK, Barber DL. Na-H Exchange-dependent Increase in Intracellular pH Times G 2 /M Entry and Transition. J Biol Chem. 2003 Nov 7; 278(45):44645–9. https://doi.org/10.1074/jbc.M308099200 PMID: 12947095

55. Casey JR, Grinstein S, Orlowski J. Sensors and regulators of intracellular pH. Nat Rev Mol Cell Biol. 2010 Jan 9; 11(1):50–61. https://doi.org/10.1038/nrm2820 PMID: 19997129